Supporting Information

Two dimensional $CuInP_2S_6$/h-BN/$MoTe_2$ van der Waals heterostructure phototransistor with double gate control

Sina Li[1,3*],Junjie Zhou[4],Jingxian Xiong[6],Sixian Yang[1,3],Jielian Zhang[1,3],Weijun Fan[5*],Jingbo Li[2*]

[1]School of Semiconductor Science and Technology, South China Normal University, Foshan 528225, P.R. China

[2]College of Optical Science and Engineering, Zhejiang University, Hangzhou 310027, China

[3]Guangdong Provincial Key Laboratory of Chip and Integration Technology, Guangzhou 510631, P.R. China

[4]School of Materials and Energy, Guangdong University of Technology, Guangzhou 510006, P.R. China

[5]School of Electrical and Electronic Engineering,Nanyang Technological University

[6]Frontier Interdisciplinary College, National University of Defense Technology, Changsha 410000, P.R. China.

Corresponding author: lisina@m.scnu.edu.cn, EWJFan@ntu.edu.sg and jbli@semi.ac.cn

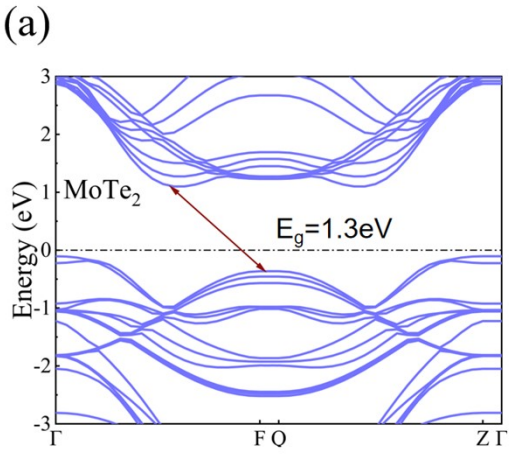

Figure S1. (a)Band structures of bulk WSe_2 based on first-principles calculations.

Density functional theory (DFT) calculations are performed utilizing the Vienna Ab initio Simulation Package (VASP).[1,2] The exchange-correlation function utilized in this investigation employs the Perdew-Burke-Ernzerhof (PBE)[3] functional within the framework of the generalized gradient approximation (GGA)[4].

1. G. Kresse, and J. Furthmüller, Phys. Rev. B 54, 11169 (1996).
2. G. Kresse, and J. Furthmüller, Comput. Mater. Sci. 6, 15 (1996).
3. J. P. Perdew, K. Burke, and M. Ernzerhof, Phys. Rev. Lett. 77, 3865 (1996).

4. P. E. Blöchl, Phys. Rev. B 50, 17953 (1994).

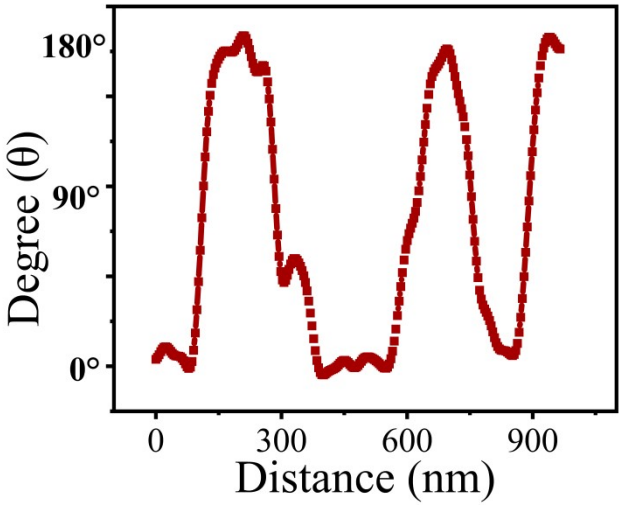

Figure S2. Along the line cutting the layered CIPS, a clear phase difference of 180 °was observed in each region.

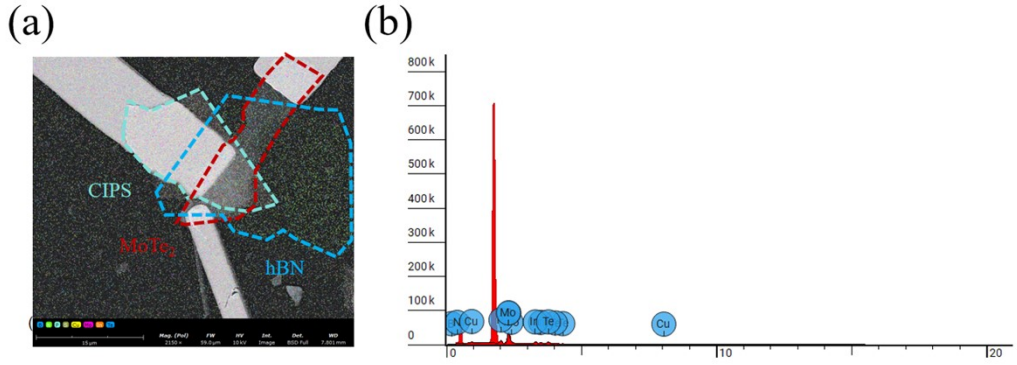

Figure S3.(a)The pseudo-color scanning electron microscopy (SEM) image.(b)The energy-dispersive X-ray spectroscopy (EDS) energy spectrum of the device.

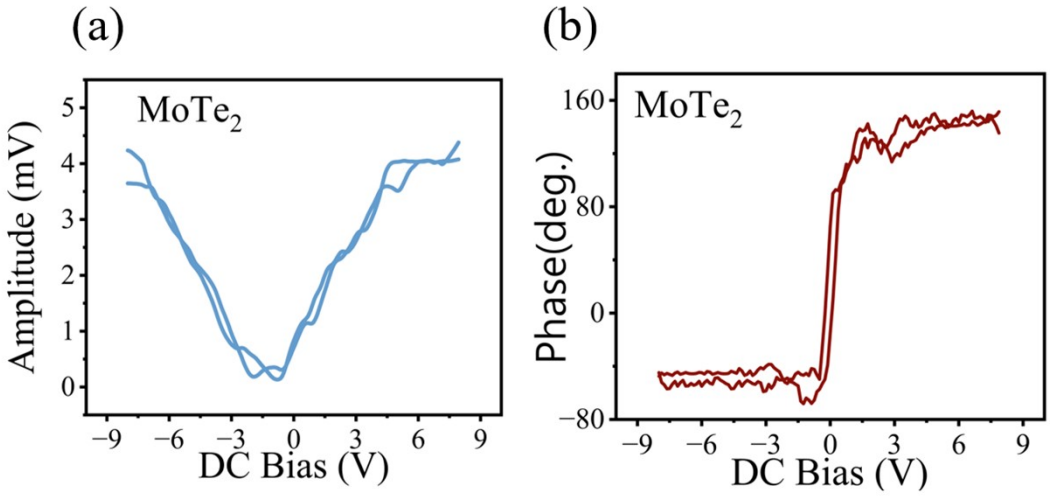

Figure S4.(a) The amplitude versus phase data of the $MoTe_2$ film.(b)The piezoresponse force

microscopy (PFM) phase versus sample bias characteristics of the $MoTe_2$ film.

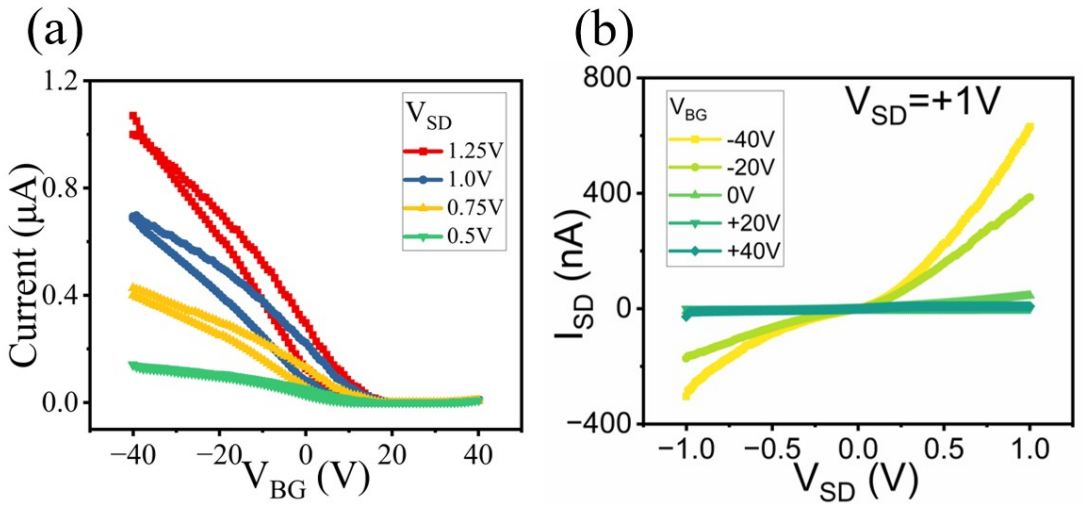

Figure S5.(a)The transfer of CIPS/hBN/$MoTe_2$ based on back gate in different bias from 0.5 to 1.25 V.(b)The output of CIPS/hBN/$MoTe_2$ in different back gate from -40 to 40V.

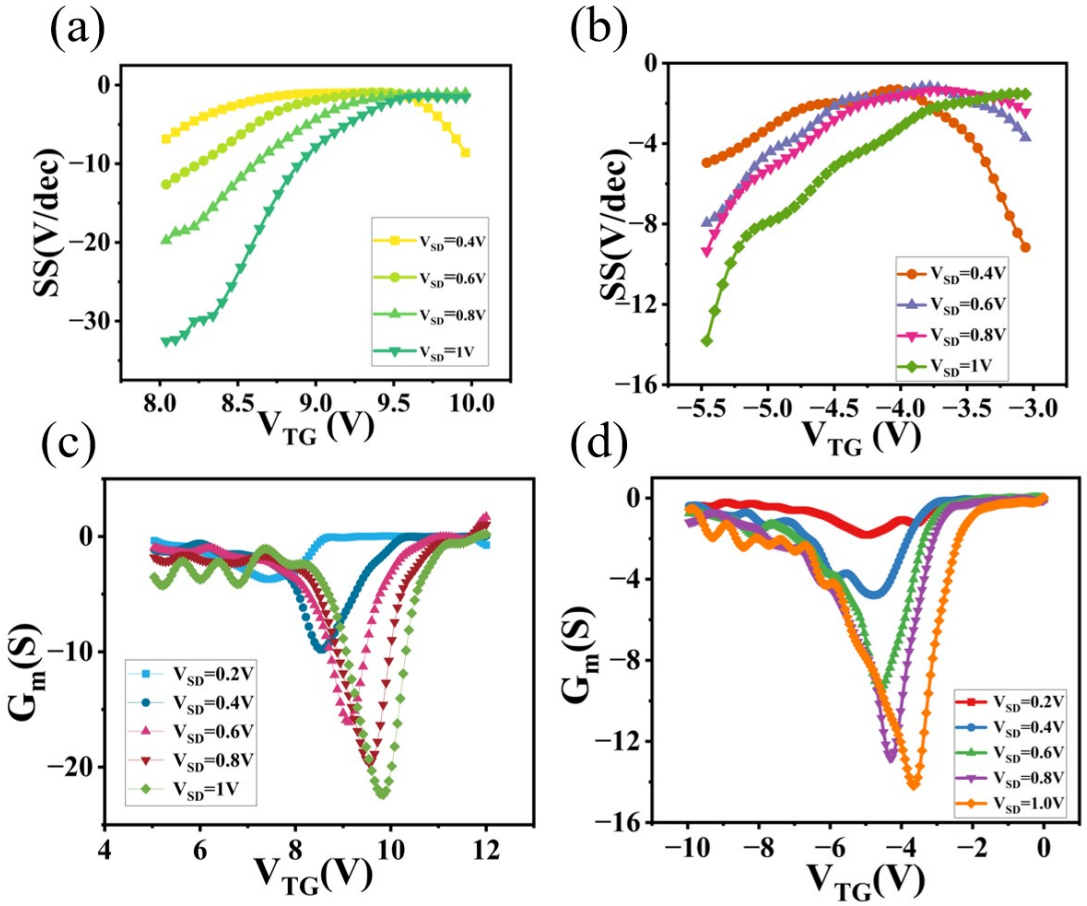

Figure S6.(a)The SS as function of positive of V_{TG} in different V_{SD} from 0.4 to 1 V.(b)The SS as function of reverse of V_{TG} in different V_{SD} from 0.4 to 1 V.(c)Transconductance(G_m) of the device as function of positive of V_{TG} in different V_{SD} from 0.4 to 1 V. (d)Transconductance(G_m) of the

device as function of reverse of V_{TG} in different V_{SD} from 0.4 to 1 V.

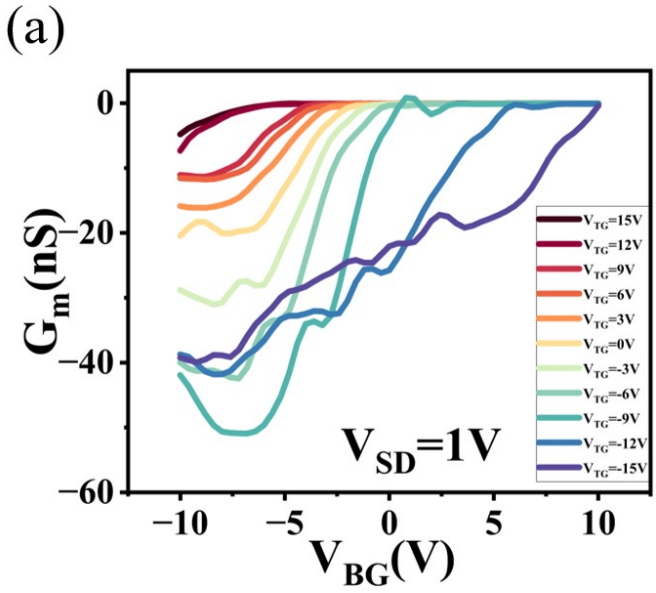

Figure S7.Transconductance of the device as function of V_{BG} at different V_{TG} (from -15 to 15V)

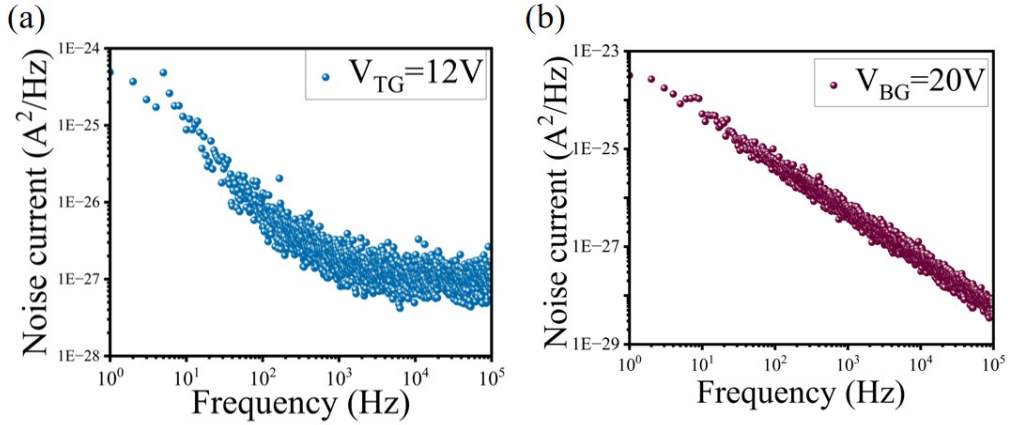

Figure S8. (a-b) The noise spectral densities of the $CuInP_2S_6$/hBN/$MoTe_2$ device recorded at V_{TG}=12V and V_{BG}=20V.

Table 1: Comparisons with other reported ferroelectric photodetectors in this work.

Device	Wavelength (nm)	Bias (V)	Gate(V)	R (mA/W)	D* (Jones)	τ (ms)	Refs.
P(VDF-TrFE)/MoTe2	1060	1	0	16.4	1.94×10^{8}	1.4/1.3	[1]
Gan/PZT/ITO	405	0	0	176	2.36×10^{13}	0.52	[2]

Gr/h-BN/InSe	637	4	0	1.18×10^{-2}	1.74×10	/0.58 15/5	[3]
GaN HEMT	365	7	-3	1.11×10^{5}	-	120/8300	[4]
InGaZnO/HfZrO	395	2	-	7.1×10^{5}	5.4×10^{12}	40/10	[5]
ZnO/PVDF	375	1	-	3.8×10^{5}	4.4×10^{15}	280	[6]
$CuInP_2S_6$/hBN/$MoTe_2$	635	1	12	6.76×10^{3}	5.67×10^{11}	1.18/1.0	This work

[1] Hai, H.; Wang, Xu.; Wang, P.; Wu, G.; Chen,Y.; Meng, C.; Liao,L.; Wang,J.; Hu,W.;Ferroelectric polymer tuned two dimensional layered $MoTe_2$ photodetector. RSC Advances, **2016**(6) 87416-87421.

[2]Chen, Z.; Lin, X.; Lin, S.; Ren, J.; Wan, L.; Peng, B.; Inverted-Structural Self-Powered Gan/PZT/ITO UV Photodetector Enhanced by Ferroelectric Modulation. *Adv. Electron. Mater*. **2024** (10) 2300588.

[3] Wang, B.; Ye, L.; Yin, H.; Ferroelectrically tuned tunneling photodetector based on graphene/h-BN/In_2Se_3 heterojunction[J].*Optical Materials*, **2024** (150)115264.

[4] Zhu,Y.; Li, Q.; Yang, Z.; Wang, C.; Wei; Z.; Research on photosensitive gate ferroelectric integrated GaN HEMT photodetector. *AIP Advances* **2021** (3) 035019.

[5] Y. Liu, Chen, W.; Zhao, L.; Guo, J.; Yang, C.; Wang, X. ; Huang, W.; Ren, T.; Xu,J.; Plasmon-Enhanced InGaZnO Ultraviolet Photodetectors Tuned by Ferroelectric HfZrO. *Adv. Electron. Mater*. **2019**(5) 1900588.

[6] Wang, P.; Wang, Y.; Ye, L.; Wu, M.; Xie, R.; Wang, X.; Chen, X.; Fan, Z.; Wang, J.; Hu, W.; Ferroelectric Localized Field-Enhanced ZnO Nanosheet Ultraviolet Photodetector with High Sensitivity and Low Dark Current. *Small* **2018** (14) 1800492.